Formation and characterisation of the silver hydride nanocluster cation $[Ag_3H_2((Ph_2P)_2CH_2)]^+$ and its release of hydrogen

Marion Girod,[a,b] Marjan Krstić,[c] Rodolphe Antoine,[a,d] Luke MacAleese,[a,d] Jérome Lemoine,[a,b] Athanasios Zavras,[e] George N. Khairallah,[e] Vlasta Bonačić-Koutecký,*[c,f] Philippe Dugourd,*[a,d] and Richard A. J. O'Hair,*[e]

Dedicated to the memory of Prof. Oliver Hampe

Abstract: Multistage mass spectrometry and density functional theory (DFT) were used to characterise of the small silver hydride nanocluster, $[Ag_3H_2L]^+$ (where L = $(Ph_2P)_2CH_2$) and its gas-phase unimolecular chemistry. Collision-induced dissociation (CID) yields $[Ag_2HL]^+$ as the major product while laser-induced dissociation (LID) proceeds via H_2 formation and subsequent release from $[Ag_3H_2L]^+$, giving rise to $[Ag_3L]^+$ as the major product. Deuterium labelling studies on $[Ag_3D_2L]^+$ prove that the source of H_2 is from the hydrides and not from the ligand. Comparison of TDDFT absorption patterns obtained for the optimised structures with action spectroscopy results allows assignment of the measured features to structures of precursors and products. Molecular dynamics "on the fly" reveal that AgH loss is favoured in the ground state, but H_2 formation and loss is preferred in the first excited state S_1, in agreement with CID and LID experimental findings. This indicates favourable photo-induced formation of H_2 and subsequent release from $[Ag_3H_2L]^+$, an important finding in context of metal hydrides as a hydrogen storage medium, which can subsequently be released by heating or irradiation with light.

Introduction

Hydrogen continues to be an attractive source of clean, renewable energy, since combustion produces water as a sole byproduct, thereby overcoming challenges associated with CO_2 emissions from traditional hydrocarbon sources.[1] The widespread use of hydrogen is hampered due to the challenge of safely storing and transporting it in its natural gaseous state.[1,2] Notwithstanding the issue of H% weight content,[3] metal hydrides have long attracted attention as a storage medium for hydrogen, which can subsequently be released by heating or via irradiation with light.[4]

Silver hydrides are key intermediates in a number of reactions involving organic substrates[5] and several silver hydrides have been recently isolated and structurally characterised via X-ray crystallography.[6] In one such study, hydrogen evolution from $[(LAg)_2H]^+$ (where L = N-heterocyclic carbene ligand 1,3-bis(2,6-diisopropylphenyl)imidazolin-2-ylidene) was observed, but the precise mechanism for H_2 formation is unknown.[6e] Gas-phase studies on mass selected silver hydride clusters allow their structure[7] and reactivity[8] to be directly probed. Here we present one of the first examples of the use of multistage mass spectrometry experiments to probe the formation of hydrogen from a small silver hydride nanocluster, $[Ag_3H_2L]^+$ (where L = bis(diphenylphosphino)methane, $(Ph_2P)_2CH_2$, DPPM) in the gas-phase.[9,10] Collision-induced dissociation (CID) and laser-induced dissociation (LID) were used to activate the cluster in order to examine its fragmentation reactions.[11] Structures of precursor and product ions were identified by the combination of action spectroscopy and Density Functional Theory (DFT), while molecular dynamics (MD) was used to identify H_2 formation mechanisms both in ground and excited states.

Results and Discussion

Gas-phase "synthesis" of $[Ag_3H_2L]^+$

The ESI mass spectrum of silver hydride clusters synthesised in solution is displayed in Figure 1a. Multistage (MS^n) CID of $[Ag_{10}H_8L_6]^{2+}$ (*m/z* 1695) resulted in sequential ligand loss, eq. 1 (MS^2, n=6; MS^3, n=5, data not shown). Isolation of $[Ag_{10}H_8L_4]^{2+}$ (*m/z* 1312) followed by another stage of CID, leads amongst others, to a series of even-electron, singly charged ligated silver hydride fragment ions arising from fission of the cluster core (Figure 1b). Some of these are complementary fragment ions arising from direct core fission (e.g. $[AgL_2]^+$ and $[Ag_9H_8L_2]^+$, eq. 2) while others arise from the initial loss of a ligand (e.g. $[Ag_3H_2L]^+$ and $[Ag_7H_6L_2]^+$, eq. 3).

$$[Ag_{10}H_8L_n]^{2+} \rightarrow [Ag_{10}H_8L_{n-1}]^{2+} + L \quad (1)$$

$$[Ag_{10}H_8L_4]^{2+} \rightarrow [AgL_2]^+ + [Ag_9H_8L_2]^+ \quad (2)$$

$$\rightarrow [Ag_3H_2L]^+ + [Ag_7H_6L_2]^+ + L \quad (3)$$

[a] *Dr M. Girod, Dr R. Antoine, Dr L. MacAleese, Prof. J. Lemoine, Prof. P. Dugourd*
Université of Lyon, 69622, France
E-mail: philippe.dugourd@univ-lyon1.fr
[b] *Dr M. Girod, Prof J. Lemoine,*
Institut des Sciences Analytiques, Université Lyon 1, CNRS UMR 5280 Lyon, France
[c] *Mr M. Krstić, Prof. V. Bonačić-Koutecký*
Interdisciplinary Center for Advanced Science and Technology (ICAST) at University of Split, Split, Croatia
[d] *Dr R. Antoine, Dr L. MacAleese, Prof. P, Dugourd*
Institut Lumière Matière, Université Lyon 1, CNRS UMR 5306, Lyon, France
[e] *A. Zavras, Dr. G. N. Khairallah, Prof. R. A. J. O'Hair*
School of Chemistry, University of Melbourne, Victoria, Australia
E-mail: rohair@unimelb.edu.au
[f] *Prof. V. Bonačić-Koutecký*
Humboldt-Universität Berlin, Institut für Chemie, Berlin, Germany
E-mail: vbk@cms.hu-berlin.de

Supporting information for this article is available on the WWW under http://dx.doi.org.10.1002/chem.xxxxxxxxx.

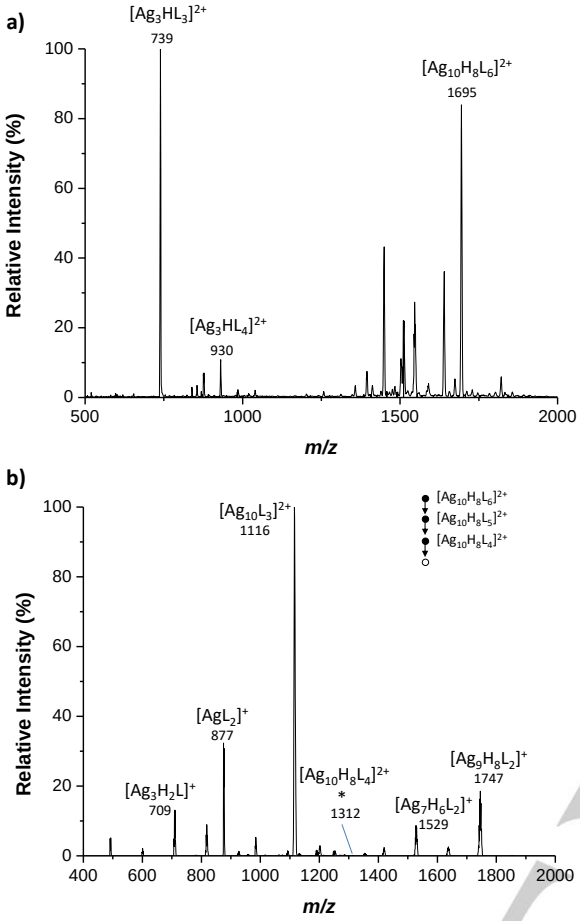

Figure 1. a) Full ESI/MS of silver hydride nanocluster ions synthesized from reaction of $AgNO_3$ with $NaBH_4$. b) MS^4 CID spectrum of $[Ag_{10}H_8L_4]^{2+}$ ion (*m/z* 1312), which was mass selected with a window of 10 Th to allow isolation of the full distribution of ^{107}Ag and ^{109}Ag isotopes. A NCE of 10% was used to dissociate the cluster and the *m/z* values of the products ions indicate the most intense peak in the cluster as a result the various combination of the silver (I) isotopes. A * indicates the mass selected precursor ion.

Gas-phase fragmentation of $[Ag_3H_2L]^+$ under CID and LID conditions

$[Ag_3H_2L]^+$ is the smallest DPPM ligated silver hydride cluster with the Ag_3 subunit and was selected for further experiments. Under CID conditions, the dominant product ion observed is $[Ag_2HL]^+$, formed via the loss of AgH (eq. 4) (Figure 2a). The next most abundant ion is $[AgL]^+$, which could arise from the loss of two AgH (eq. 5) or the dimer (eq. 6). Minor channels due to the formation of H_2 (eq. 7) and Ag_3H (eq. 8) are also observed. In contrast, the major product of LID arises from dehydrogenation (eq. 7) (Figure 2b), with minor products $[Ag_2HL]^+$, $[Ag_2L]^+$ and $[AgL]^+$ also occurring. All fragmentation channels were confirmed by substituting $NaBH_4$ for $NaBD_4$ during the synthesis and using the $[Ag_3D_2L]^+$ deuterium labelled cluster (Supplementary Figure S1). These experiments highlight that DPPM is not the source of the H for either the AgH losses under CID conditions (Figure S1a) or H_2 formation and release under LID (Figure S1b).

$$[Ag_3H_2L]^+ \rightarrow [Ag_2HL]^+ + AgH \quad (4)$$
$$\rightarrow [AgL]^+ + 2AgH \quad (5)$$
$$\rightarrow [AgL]^+ + Ag_2H_2 \quad (6)$$
$$\rightarrow [Ag_3L]^+ + H_2 \quad (7)$$
$$\rightarrow [L+H]^+ + Ag_3H \quad (8)$$

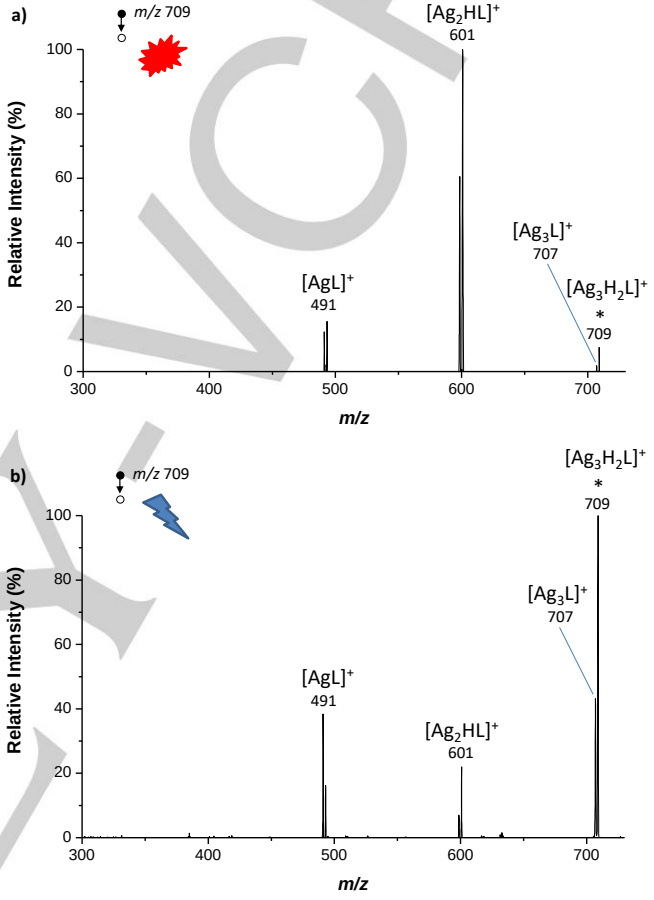

Figure 2. MS^5 spectra showing the fragmentation of the $[Ag_3H_2L]^+$ ion (*m/z* 709) under conditions of: a) CID with a NCE of 25%. b) Laser-induced dissociation (LID) at 260 nm with 5 laser shots. A * designates the mass selected precursor ions. A window of 1.3 Th was used to isolate a single peak from the isotope cluster, corresponding to $[^{107}Ag_2{}^{109}AgH_2L]^+$.

Gas-phase reaction of $[Ag_3L]^+$ with hydrogen

We also examined the reaction of $[Ag_3L]^+$ with hydrogen, to establish whether $[Ag_3H_2L]^+$ could be regenerated (eq. 9). No reaction was observed under a range of conditions including near thermal reaction conditions (reaction times of up to 10 s), as well as activation of $[Ag_3L]^+$ by collisions of the mass selected precursor with the neutral bath gas (reaction time of 100 ms) or laser irradiation at either 265 or 310 nm (reaction times of 500 ms) in the ion trap (Supplementary Figure S2). The lack of reactivity under "near thermal" conditions [12] for the given concentration of H_2 and the reaction times examined establishes an upper limit for the rate of ca. $2x10^{-16}cm^3.molecule^{-1}.s^{-1}$, which corresponds to a reaction efficiency of 10^{-5} %.[13] This is

consistent with DFT calculations, which reveal that while eq.9 is exothermic by 0.37 eV, it has a barrier of 0.61 eV (Supplementary Figure S3).

$[Ag_3L]^+ + H_2 \rightarrow [Ag_3H_2L]^+$ (9)

Structural and optical properties of $[Ag_3H_2L]^+$

Comparison of the action spectrum and calculated TD-DFT spectrum for the lowest energy structure, shown in Figure 3a, confirms the structural properties of $[Ag_3H_2L]^+$, which possesses a Ag_3H_2 planar subunit that is attached to the DPPM ligand via both phosphorous atoms. It is worth noting that the equilibrium structure of S_1 differs from the ground state structure (see Supplementary Figure S4), with the two hydrogens being inserted into two Ag-Ag bonds. The absorption features are characterised by two bands centred at 250 nm with a shoulder at 270 nm. Corresponding TD-DFT transitions to S_1 and S_8 excited states, which are dominant in the wavelength region, are characterised mainly by the transitions within Ag_3H_2 – P_2 subunits as shown in Figure 3b.

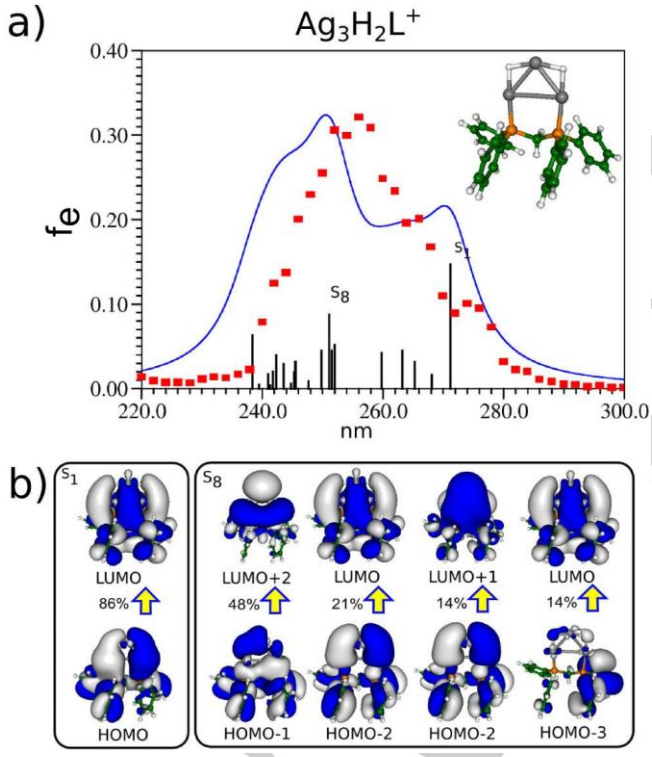

Figure 3. a) Photo-fragmentation spectrum (red dotted line) and calculated TD-DFT spectrum (the blue full line corresponds to Lorentzian broadening with half width of 10 nm, the black vertical lines correspond to values of oscillator strength f_e) for the lowest energy structure of $[Ag_3H_2L]^+$, b) analysis of leading excitations contributing to the most intense transitions (to S_1 and S_8 states) (cut-off for MOs is 0.04, minus and plus are labelled by blue and grey colours, respectively)

To confirm structural assignment for $[Ag_3L]^+$, the main product after photoexcitation of $[Ag_3H_2L]^+$ (eq. 7), action spectroscopy as well as complementary calculations were performed. The main fragmentation channel after collision and excitation of $[Ag_3L]^+$ is the loss of Ag_2 (eq. 10, Supplementary Figure S5). The absorption features are characterised by two bands between 200 and 300 nm (Figure 4a). The calculated lowest energy transition at 380 nm is not accessible experimentally. The main features are reproduced experimentally while the exact positions are slightly red-shifted (Figure 4a). This might be caused by the conformational structure of the DPPM ligand in which the relative position of the phenyl rings substantially influences the spectroscopic pattern (*vide infra*). Analysis of the dominant transitions (Figure 4b) shows significant participation of excitations within the metallic subunit.[14]

$[Ag_3L]^+ \rightarrow [AgL]^+ + Ag_2$ (10)

Structural and optical properties of the protonated ligand

The experimental and calculated absorption properties of $[L+H]^+$ were examined as a reference point (Figure 4c). The structure shown in the inset of Figure 4c, which matches the conformation of the neutral ligand determined via X-ray crystallography,[15] is comparable to the theoretically found lowest-energy structure. However, the relative position of the phenyl rings substantially influences the absorption features (Supplementary Figure S6). The spectrum of $[L+H]^+$ (Figure 4c) is characterised by a dominant transition at 260 nm with smaller shoulders at around 240 and 300 nm. The analysis of leading excitations for intense transition (Figure 4d) illustrates that excitations occur, either between left and right phenyl rings, or bottom and up phenyl rings. The main fragmentation channel for this ion after UV excitation is the cleavage of the C-P bond (eq. 11) (Supplementary Figure S7), which is not observed when it is complexed with silver.

$[Ph_2PCH_2P(H)Ph_2]^+ \rightarrow [Ph_2PCH_2]^+ + Ph_2PH$ (11)

Molecular dynamics for the fragmentation of $[Ag_3H_2L]^+$ in the ground state

The experimental findings described above have been confirmed by MD simulations, which show that in the ground state (S_0) loss of AgH occurs (eq. 4, Figure 5a) and that the experimentally observed product $[AgL]^+$ is likely to be formed by loss of 2 AgH (eq. 5, Figure 5b) as well as Ag_2H_2 (eq. 6, Figure 5c). The fragmentation channel leading to H_2 formation and release was also found (eq. 7, Figure 5d). The MD simulations have been carried out at 2400 K, confirming the high stability of the precursor ion. At this high temperature, the observed fragmentation channels are initiated by Ag-Ag bond breaking that can be qualitatively explained by the nature of HOMO, which contains a node between the Ag-Ag, bond as shown in Figure 3. Note that fragmentation of the bound DPPM ligand was not observed experimentally but that the MD simulation at high temperature indicates that fragmentation of the DPPM ligand occurs via C-P bond activation (Figure 5e). The MD simulations suggest that loss of the Ag_3H_2 subunit (Figure 5f) might occur, and this may be related to the experimentally observed formation of $[L+H]^+$ (eq. 8).

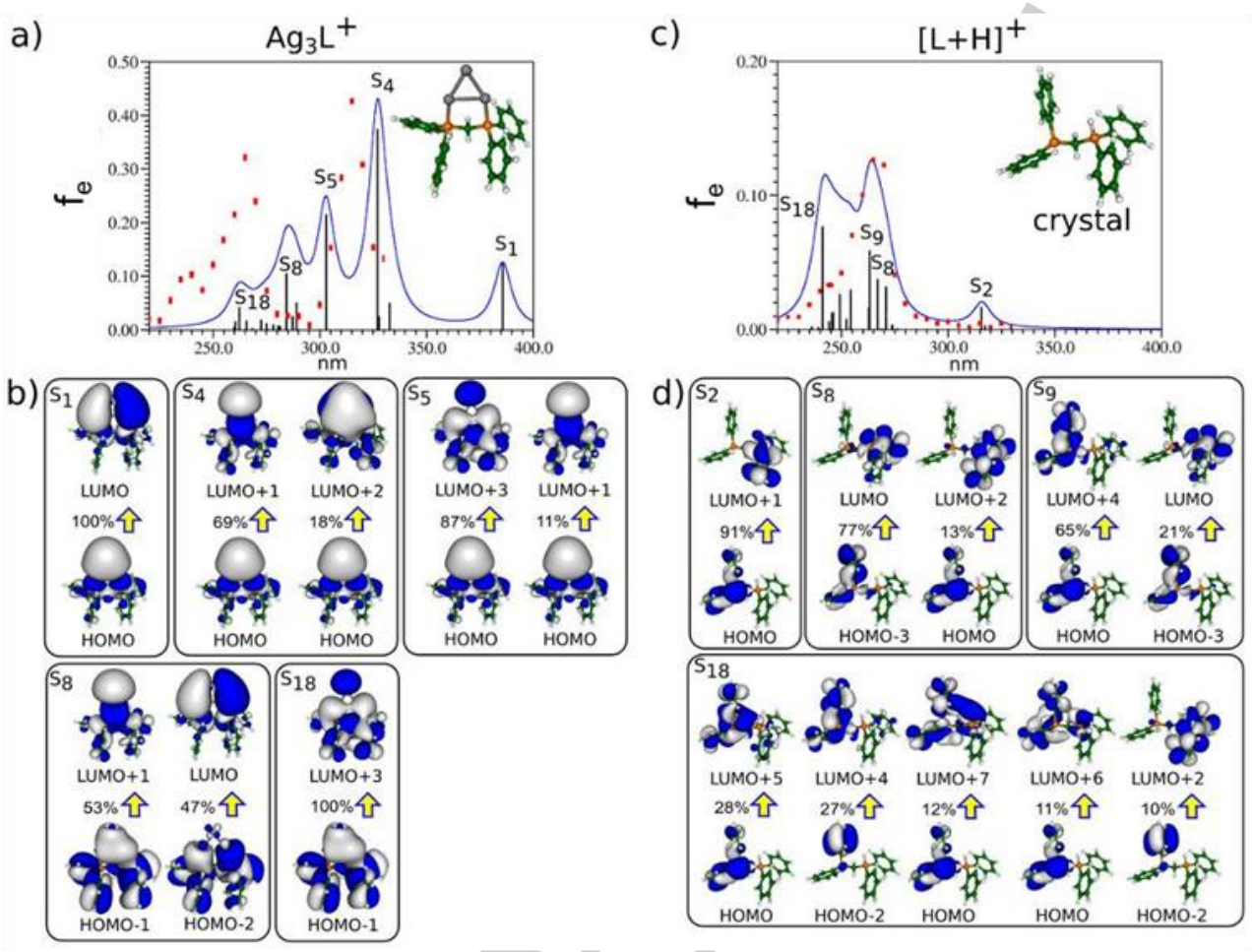

Figure 4. a) Photo-fragmentation spectrum (red dotted line) and calculated TD-DFT spectrum (the blue full line corresponds to Lorentzian broadening with half width of 10 nm, the black vertical lines correspond to values of oscillator strength f_e) for the lowest energy structure of $[Ag_3L]^+$, b) analysis of leading excitations contributing to the most intense transitions, c) spectra for the conformation of $[L+H]^+$ that matches the crystal structure of the neutral ligand (for labelling cf. a) and d) analysis of excitations contributing to the most intense transitions (cut-off for MOs is 0.04, minus and plus are labelled by blue and grey colours, respectively)

Molecular dynamics for the fragmentation of $[Ag_3H_2L]^+$ in the first excited state

The MD "on the fly" has been also carried out in the first excited state (S_1) and compared with LID experimental results. The leading excitation for the S_1 state (cf. Figure 3) is HOMO→LUMO where LUMO contains two nodes separating each H from Ag_3 indicating qualitatively that formation of H_2 in the first excited state might occur. Indeed, in the S_1 state two fragmentation channels involving dissociation by the formation of H_2 (cf. Figure 6a) and AgH (cf. Figure 6b) have been found by MD simulations and LID measurements (cf. Figure 2). In the latter, H_2 dissociation is dominant as expected due to the nature of S_1 state. The mechanism for H_2 formation involves weakening of Ag-Ag bonds at the beginning of dynamics, which corresponds to a motion towards the equilibrium structure in S_1 state. This induces formation and subsequent release of H_2 and deformation of Ag_3 subunit. This is not the case for the fragmentation of H_2 in the ground state (cf. Figures 5 and 6). In contrast, the mechanism for fragmentation via AgH loss in the ground and excited state are less distinguishable (cf. Figures 5a and 6b). The structure and nature of S_1 favours hydrogen formation and subsequent release, which explains why hydrogen loss is the most abundant relaxation channel after photo-excitation.

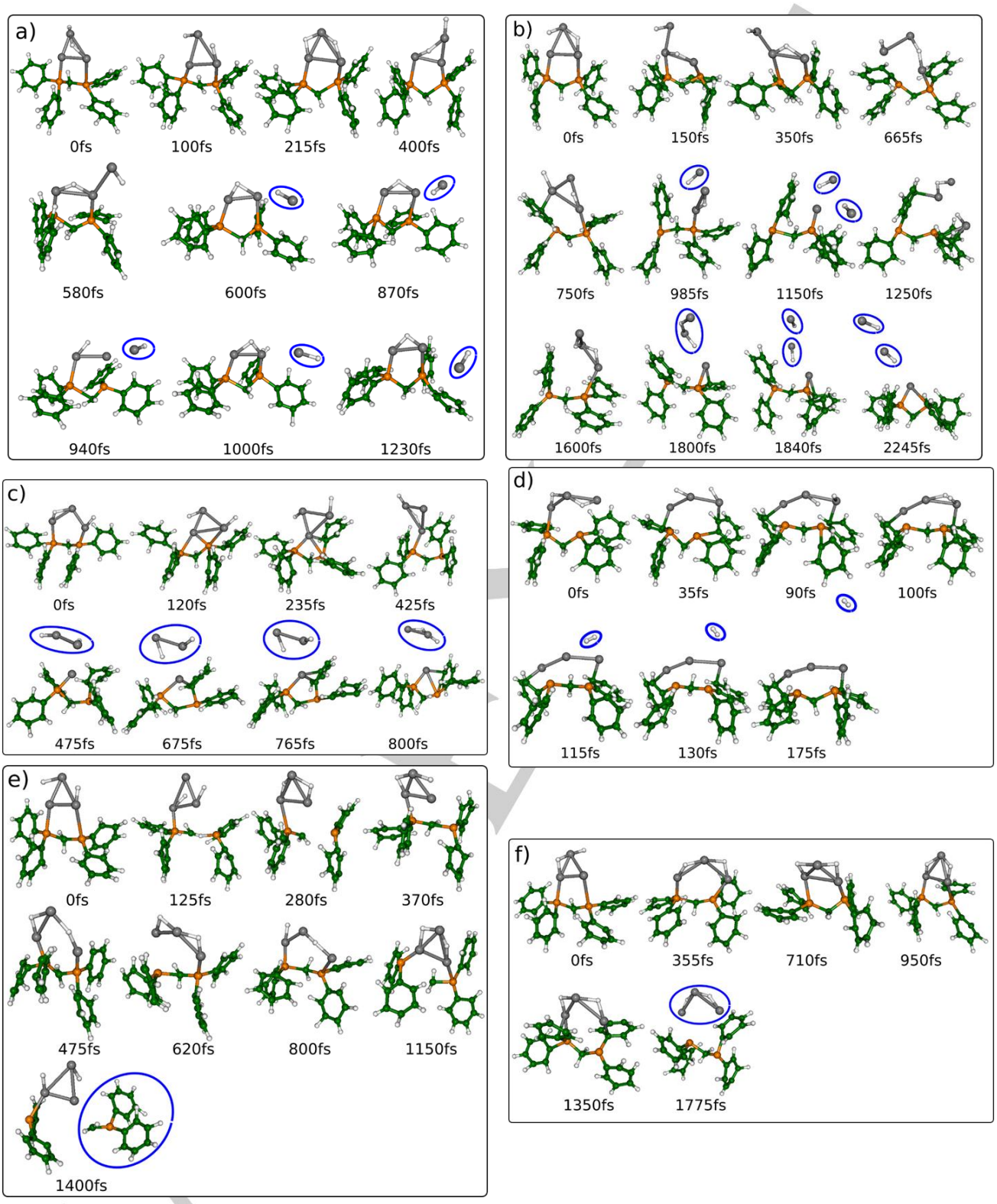

Figure 5. Snapshots of the MD "on the fly" using the DFT method with PBE functional and TZVP AO basis set in the electronic ground state S_0 from selected trajectory at high temperature (2400K) yielding the following fragmentation channels of $[Ag_3H_2L]^+$: a) $Ag_3H_2L^+ \rightarrow Ag_2HL^+ + AgH$, b) $Ag_3H_2L^+ \rightarrow AgL^+ + 2AgH$, c) $Ag_3H_2L^+ \rightarrow AgL^+ + Ag_2H_2$, d) $Ag_3H_2L^+ \rightarrow Ag_3L^+ + H_2$, e) $Ag_3H_2L^+ \rightarrow Ag_3H_2(PPh_2)^{+\bullet} + {}^{\bullet}CH_2PPh_2$, f) $Ag_3H_2L^+ \rightarrow L + Ag_3H_2^+$.

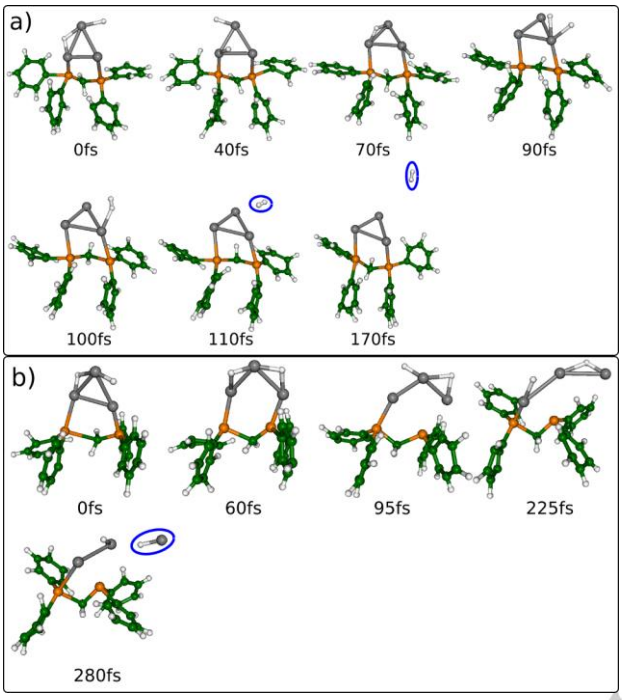

Figure 6. Snapshots of the MD "on the fly" using DFT with PBE functional and TZVP AO basis set in the first electronic excited state S_1 from selected trajectory at high temperature (2400K) of $[Ag_3H_2L]^+$ yielding the following fragmentation channels: a) $[Ag_3H_2L]^+ \rightarrow [Ag_3L]^+ + H_2$, b) $[Ag_3H_2L]^+ \rightarrow [Ag_2HL]^+ + AgH$

Conclusions

While transition metal hydrides are unlikely to be used as hydrogen storage materials due to their low H% weight content, there is continued interest in the use of transition metal compounds to catalyze the decomposition of other compounds with higher H% weight content.[3,16] Since these latter processes are likely to involve the formation of transition metal hydrides, our findings are important as they reveal a key difference in the ground versus excited state dissociation of a hydride containing nanocluster. Photo-activation leads to excitation within the Ag_3H_2 core involving a geometry change, which weakens the silver-hydrogen bonds. This is a consequence of the difference between the geometry in ground and excited states of the complex. This finding may be a general route for the photo-release of hydrogen in ligated metallic hydrides. Stabilization of the metal cluster by the ligands may favour hydrogen release, which was not observed for example after UV photo-excitation of $[Li_3H_2]^+$.[17] Current work is underway to examine the decomposition of the promising hydrogen storage material formic acid catalyzed by ligated silver nanoclusters.[18]

Finally, the observation of photo-induced hydrogen formation from an ionic silver hydride nanocluster is also important as it: (i) is a model for a photo-induced reductive elimination, which is a likely to be a key step in bond formation from reactive intermediates involved in photo-catalysis by metal clusters;[19] (ii) provides a direct link between ionic silver clusters and metallic silver clusters. The reactions of sodium borohydride with silver salts in the presence of ligands is widely used to generate silver nanoclusters and silver nanoparticles.[20] The vast majority of these studies fail to consider the possibility of forming silver hydride containing species, and while evolution of hydrogen is formulated as a key reaction during the reduction of silver salts by sodium borohydride,[21] no-one appears to have considered light- or thermal-induced reductive elimination of hydrogen from silver hydride nanoclusters or nanoparticles.

Experimental Section

Chemicals

Silver(I) trifluoroacetate, bis(diphenylphosphino)methane (DPPM), sodium borohydride and sodium borodeuteride were purchased from Sigma Aldrich (Saint Quentin Fallavier, France). Chloroform and methanol were HPLC grade sourced from Sigma Aldrich. Helium seeded with 1% hydrogen gas used for the ion-molecule reactions was purchased from Air Liquide (Pierre-Bénite, France). All chemicals were used as received. $[Ag_{10}H_8L_6]^{2+}$ and $[Ag_{10}D_8L_6]^{2+}$ were synthesized in solution by the reaction of a mixture of silver(I) trifluoroacetate (2.2 mg, 0.010 mmol) and bis(diphenylphosphino)methane (3.8 mg, 0.010 mmol) with sodium borohydride (2.0 mg, 0.050 mmol) and sodium borodeuteride (2.1 mg, 0.050 mmol) respectively in 20 mL MeOH:$CHCl_3$ (1:1) as described previously [6d].

Mass spectrometry

Solutions of $[Ag_{10}H_8L_6]^{2+}$ or $[Ag_{10}D_8L_6]^{2+}$ prepared as outlined above were further diluted with methanol to a concentration of around 75 µM and introduced into a modified quadrupole linear ion trap mass spectrometer (LTQ, Thermo Fisher Scientific, San Jose, CA, USA) via electrospray ionization (ESI) using a syringe pump set to a flow rate of 5 µL.min-1. The typical ESI conditions used were: spray voltage, 4.2 – 5.0 kV, capillary temperature, 250°C, nitrogen sheath gas pressure, 5 (arbitrary units), capillary voltage 15 V. The modification to the mass spectrometer consists of the installation of a quartz window fitted on the rear of the MS chamber to allow the introduction of a laser beam.[22] The laser is a nanosecond frequency-doubled tuneable PantherTM EX OPO (Optical Parametric Oscillator) laser pumped by a SureliteTM II Nd:YAG laser (both from Continuum, Santa Clara, CA, USA). The repetition rate of the laser was 10 Hz. The laser beam passes through two diaphragms (1 mm diameter), lenses and a mechanical shutter electronically synchronized with the mass spectrometer, after which it is injected on the axis of the linear trap. The laser power was monitored with a power meter located just before the injection in the ion trap. The mechanical shutter is used to synchronize the laser irradiation with the trapping of the ions. To perform laser irradiation for a given number of laser pulses, we add in the ion trap radio frequency (RF) sequence an MS^n step with an activation amplitude of 0% and a reaction time of 500 ms, during which the shutter located on the laser beam is opened. The activation q value was set to 0.25. An *m/z* window of 1.3 Th was applied for ion precursor isolation which contained the 2 x ^{107}Ag and 1 x ^{109}Ag isotopes. For CID experiments the normalized collision energy was set to 15% and the activation time to 100 ms.

For action spectroscopy, mass spectra were recorded after laser irradiation as a function of the laser wavelength. At each laser wavelength from 220 nm to 330 nm (with a 2 nm step), a laser-normalized yield of photo-fragmentation is deduced from the mass spectrum through

$$\sigma = \ln((parent + daughter)/parent)/ \Phi \quad (11)$$

Where Φ is the laser fluence, parent is the intensity of the precursor ion, and daughter represents the intensity of the product ion peaks. Optical action spectra were obtained by plotting the normalized yield of photo-fragmentation as a function of the laser wavelength.

To assess the optical properties of $[Ag_3L]^+$ ion, we combined a BrillantB Nd:YAG laser (from Quantel, Les Ulis, France) to the OPO laser in a two colour scheme.[23] The 4th harmonic at λ=266 nm was used with a repetition rate of 20 Hz and 20 mJ/pulse. The two photon beams were spatially combined via a 266 nm dichroic mirror located ~30 cm upstream of the ion trap entrance. The 266 nm laser beam was reflected at 90° by the dichroic mirror and injected collinearly to the axis of the ion trap. The UV laser light was injected along the same ion trap axis passing through the dichroic mirror. Two electromechanical shutters, electronically synchronized with the mass spectrometer, were placed along the 266 nm laser and UV beam from the OPO and allowed to inject the 2 colour lights according to a given time sequence. For UV irradiation of $[Ag_3L]^+$ ion, we used the deuterated species, $[Ag_3D_2L]^+$ precursor ions which were first selected in MS^n, irradiated by the 266 nm UV laser for 500 ms, then the produced ion was isolated during the $MS^{(n+1)}$ stage and activated by UV from the OPO during 500 ms. Mass spectra were recorded after OPO irradiation as a function of the OPO wavelength.

For the ion-molecule reactions of $[Ag_3L]^+$ with hydrogen, the normal high purity helium bath gas was replaced with a helium cylinder seeded with 1% hydrogen. $[Ag_3L]^+$ was formed by multistage mass spectrometry experiments using CID to induce fragmentation of precursor ions, and then mass selected and stored in the ion trap with reaction times of up to 10 s.

Theory

Density functional theory (DFT) was used to determine the structural properties of the $[Ag_3L]^+$ and $[Ag_3H_2L]^+$. For this purpose the hybrid B3LYP functional[24] with TZVP atomic basis set was used for all atoms.[25] Silver atoms have been treated by Stuttgart relativistic effective core potential (RECP) with corresponding AO basis set.[26] Although the extensive search for lowest energy structures have been performed, the crystal structure of the bisdiphenylphosphinomethane ligand, $(Ph_2P)_2CH_2$, has been used as a starting reference for the relative orientation of the phenyl rings, which seem to have large influence on optical properties of their complexes with Ag_3 and H_2. For optimized structures the stationary points were characterised by calculating the harmonic vibrational frequencies. For calculations of the absorption spectra time dependent density functional method (TDDFT) with B3LYP functional and TZVP AO basis set has been employed. The fragmentation channels in the ground and excited states have been determined using molecular dynamics (MD) "on the fly" based on DFT approach with Perdew-Burke-Ernzerhof (PBE) functional[27] and resolution of identity (RI) approximation[28] due to considerably smaller computational demand. The initial conditions for the MD "on the fly" in the ground and first excited state were obtained by sampling coordinates and momenta at regular time intervals along a ground state trajectory at constant temperature in the framework of DFT method.

Acknowledgements

R.A.J.O. thanks: the Australian Research Council for financial support through the CoE program; The Université de Lyon for a visiting Professorship and the School of Chemistry at the University of Melbourne for a short term study leave. V.B.-K. and P. D. thank the CNRS NCBA international laboratory. V.B.-K. acknowledges support by the Deutsche Forschungsgemeinschaft (DFG FOR1282) and by Split-Dalmatia County.

Keywords: Silver hydride clusters•hydrogen formation•fragmentation channels•multistage mass spectrometry•optical spectra•molecular dynamics

[1] a) The Hydrogen Economy: Opportunities, Costs, Barriers, and R&D Needs. National Academy Press, **2004**; b) G. W. Crabtree, M. S. Dresselhaus, M. V. Buchanan, *Physics Today* **2004**, *57*, 39–44; c) P. Jena, *J. Phys. Chem. Lett.* **2011**, *2*, 206–211.

[2] a) L. Schlapbach, A. Züttel, *Nature* **2001**, 414, 353-358; b) F. Schüth, *Eur. Phys. J. Special Topics* **2009**, *176*, 155–166; c) M. T. Kelly, *Struct. Bond.***2011**, *141*, 169–201.

[3] For an excellent review on hydrogen storage materials, including a discussion on the "5 commandments" for the ideal hydrogen storage material, see: W. Grochala, P. P. Edwards, *Chem. Rev.* **2004**, *104*, 1283–1315.

[4] A. S. Weller, J. S. McIndoe, *Eur. J. Inorg. Chem.* **2007**, 4411–4423.

[5] a) K. Shimizu, R. Sato, A. Satsuma, *Angew. Chem. Int. Ed.* **2009**, *48*, 3982–3986; b) K. Shimizu, K. Sugino, K. Sawabe, A. Satsuma, *Chem. Eur. J.* **2009**, *15*, 2341–2351; c) K. Shimizu, A. Satsuma, *J. Jpn. Petrol. Inst.* **2011**, *54*, 347–360.

[6] a) C. W. Liu, H.-W. Chang, C.-S. Fang, B. Sarkar, J.-C. Wang, *Chem. Commun.* **2010**, *46*, 4571–4573; b) C. W. Liu, H.-W. Chang, B. Sarkar, J.-Y. Saillard, S. Kahal, Y.-Y. Wu, *Inorg. Chem.* **2010**, *49*, 468–475; c) C. W. Liu, P.-K. Liao, C.-S. Fang, J.-Y. Saillard, S. Kahal, J.-C. Wang, *Chem. Commun.* **2011**, *47*, 5831–5833; d) A. Zavras, G. N. Khairallah, T. U. Connell, J. M. White, A. J. Edwards, P. S. Donnelly, R. A. J. O'Hair, *Angew. Chem. Int. Ed.* **2013**, *52*, 8474–8474; e) B. K. Tate, C. M. Wyss, J. Bacsa, K. Kluge, L. Gelbauma, J. P. Sadighi, *Chem. Sci.* **2013**, *4*, 3068–3074; f) A. Zavras, G. N. Khairallah, T.U. Connell, J. M. White, A. J. Edwards, R. J. Mulder, P. S. Donnelly, R. A. J. O'Hair, *Inorg. Chem.* **2014,** *53*, 7429-7437.

[7] R. Mitrić, J. Petersen, A. Kulesza, M. Röhr, V. Bonačić-Koutecký, C. Brunet, R. Antoine, P. Dugourd, M. Broyer, R. A. J. O'Hair, *J. Phys. Chem. Lett.* **2011**, *2*, 548–552.

[8] a) G. N. Khairallah, R. A. J. O'Hair, *Angew. Chem. Int. Ed.* **2005**, *44*, 728–731; b) G. N. Khairallah, R. A. J. O'Hair, *Dalton Trans.* **2005**, 2702–2712; c) G. N. Khairallah, R. A. J. O'Hair, *Dalton Trans.* **2007**, 3149–3157; d) G. N. Khairallah, R. A. J. O'Hair, *Dalton Trans.* **2008**, 2956–2965; e) F. Q. Wang, G. N. Khairallah, R. A. J. O'Hair, *Int. J. Mass Spectrom.* **2009**, *283*, 17–25; f) A. J. Clark, A. Zavras, G. N. Khairallah, R. A. J. O'Hair, *Int. J. Mass Spectrom.,* **2014** http://dx.doi.org/10.1016/j.ijms.2014.07.015, in press.

[9] For an example of the gas-phase collision-induced formation and loss of H_2 from the metal hydride cluster ion $Nb_7H_8^+$ see: A. B. Vakhtin, E. M. Markin, K.-I. Sugawara, *Chem. Phys.* **2000**, *262*, 93–104.

[10] The gas-phase reactions of transition metal atomic cations with H_2 have been widely studied: a) Armentrout, P. B. *Int. Rev. Phys. Chem.* **1990**, *9*, 115–148. For examples of the gas-phase reactions of metal cluster ions with H_2 see: b) A. B. Vakhtin, K.-I. Sugawara, *J. Chem. Phys.* **2001**, *115*, 3629–3639; c) F. Liu, P. B. Armentrout, *J. Chem. Phys.* **2005**, *122*, 194320/1-194320/12.

[11] The gas-phase IR spectrum of the $Ag(H_2)^+$ complex has been recently reported: V. Dryza, E. J. Bieske, *J. Phys. Chem. Lett.* **2011**, *2*, 719–724.
[12] W. A. Donald, G. N. Khairallah, R. A. J. O'Hair, *J. Am. Soc. Mass Spectrom.*, **2013**, *24*, 811-815.
[13] Activation of the H-H bond by Ag^+ is endothermic and produces AgH+: Y.-M. Chen, J. L. Elkind, P. B. Armentrout, *J. Phys. Chem.* **1995**, *99*, 10438-10445.
[14] T. Tabarin, A. Kulesza, R. Antoine, R. Mitrić, M. Broyer, P. Dugourd, V. Bonačić-Koutecký, *Phys. Rev. Lett.* **2008**, *101*, 213001.
[15] R. A. Burrow, F. C. Wouters, L. Borgen de Castro, C. Peppe, *Acta Cryst.* **2007**, *E63*, o2559.
[16] For reviews of the metal catalyzed decomposition of formic acid for applications in hydrogen storage see: a) S. Enthaler, J. Langermann, T. Schmidt, *Energy Environ. Sci.* **2010**, *3*, 1207–1217; b) M. Grasemann, G. Laurenczy, *Energy Environ. Sci.* **2012**, *5*, 8171–8181.
[17] R. Antoine, P. Dugourd, D. Rayane, E. Benichou and M. Broyer. *J. Chem. Phys.* **1997**, *107*, 2664-2672.
[18] For a report on the gas-phase decomposition of formic acid catalyzed by magnesium hydrides see: G. N. Khairallah, R. A. J. O'Hair, *Int. J. Mass Spectrom.* **2006**, *254*, 145–151.
[19] a) R. J. Wang, T. Fujimoto, T. Shido, M. Ichikawa, *J. Chem. Soc., Chem. Comm.* **1992**, 962–963; b) Y. Negishi, *Bull. Chem. Soc. Jpn.* **2014**, *87*, 375–389.
[20] M. Wuithschick, B. Paul, R. Bienert, A. Sarfraz, U. Vainio, M. Sztucki, R. Kraehnert, P. Strasser, K. Rademann, F. Emmerling, *J. Polte, Chem. Mater.* **2013**, *25*, 4679–4689 and references cited therein.
[21] S. D. Solomon, M. Bahadory, A. V. Jeyarajasingam, S. A. Rutkowsky, C. Boritz, L. Mulfinger, *J. Chem. Educ.* **2007**, *84*, 322–325.
[22] a) V. Larraillet, R. Antoine, P. Dugourd, J. Lemoine, *Anal. Chem.* **2009**, *81*, 8410–8416. b) R. Antoine, P. Dugourd, *Phys. Chem. Chem. Phys.* **2011**, *13*, 16494–16509.
[23] L. Joly, R. Antoine, A. R. Allouche, P. Dugourd, *J. Am. Chem. Soc.* **2008**, *130*, 13832–13833.
[24] a) A. D. Becke, *J. Chem. Phys.* **1988**, *38*, 3098; b) A. D. Becke, *J. Chem. Phys.* **1993**, *98*, 5648; c) C. Lee, W. Yang, R. G. Parr, *Phys. Rev. B***1988**, *37*, 785.
[25] Schäfer, A.; Huber, H.; Ahlrichs, R. *J. Chem. Phys.* **1994**, *100*, 5829−5835.
[26] D. Andrae, U. Haeussermann, M. Dolg, H. Stoll, H. Preuss, *Theor. Chim. Acta* **1990**, *77*, 123.
[27] Perdew, J. P.; Burke, K.; Ernzerhof, M. *Phys. Rev. Lett.* **1996**, *77*, 3865−3868.
[28] Eichkorn, K.; Treutler, O.; Öhm, H.; Häser, M.; Ahlrichs, R. *Chem. Phys. Lett.* **1995**, *242*, 652−660

FULL PAPER

Experiment and theory provide the first example of photochemical triggered formation and release of hydrogen from a small metal hydride cluster in the gas-phase.

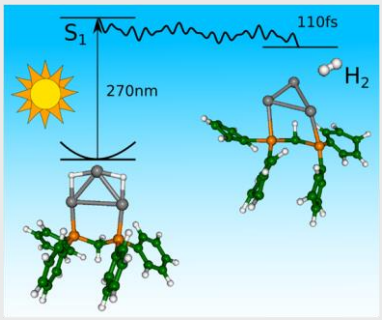

Marion Girod,[a,b] Marjan Krstić,[c] Rodolphe Antoine,[a,d] Luke MacAleese,[a,d] Jérome Lemoine,[a,b] Athanasios Zavras,[e] George N. Khairallah,[e] Vlasta Bonačić-Koutecký,[c,f] Philippe Dugourd,*[a,d] and Richard A. J. O'Hair,*[e]*

Page No. – Page No.

Formation of the silver hydride nanocluster cation $[Ag_3H_2((Ph_2P)_2CH_2)]^+$ and its release of hydrogen